



ANALYSIS OF MIXED-MODE CRACK TIP IN FUNCTIONALLY GRADED BEAMS BY USING XEFGM

Dr. Haider Khazal Mehbes
haider_khazal@yahoo.com

Dr. Hassanein Ibraheem Khalaf
hassanein.ibraheem@gmail.com

Mechanical engineering department College of Engineering
University of Basrah

ABSTRACT :-

An extended element free Galerkin method (XEFGM) has been adopted for crack propagation of for graded glass/epoxy beams (along X_1) subjected to non-proportional four point bending. The incompatible interaction integral method and the sub-triangle technique for enhancing the gauss quadrature accuracy near the crack are employed to calculate the stress intensity factors. Numerical simulations have proved that XEFGM provides accurate results by less number of nodes (DOFs) in comparison with the conventional FEM under mixed-mode and non-proportional loading. MATLAB codes are used in obtaining the results of this research. The results have shown good the reliability, stability, and efficiency of present XEFGM and good agreements with the experimental works of crack propagation with using less nodes in compare with the relevant references.

KEYWORDS : crack propagation, functionally graded materials, stress intensity factors,

تحليل الشرخ المركب في العوارض المتدرجة وظيفيا باستخدام الطريقة اللاشبيكية XEFGM

المدرس الدكتور حيدر خزعل محبس
قسم الهندسة الميكانيكية
كلية الهندسة / جامعة البصرة
المدرس الدكتور حسنين ابراهيم خلف

الخلاصة :-

تم اعتماد الطريقة اللاشبيكية المطورة (XEFGM) لمحاكاة نمو الشروخ في عوارض الزجاج-الايبوكسي المتدرجة (حول محور X_1) تحت حمل انحناء رباعي النقاط . طريقه التكامل التفاعلي غير المتوافق تم استخدامها مع تقنية غاوس للمثلثات الفرعية في توزيع نقاط التكامل عند منطقه الشرخ لحساب معامل تركيز الإجهاد. وقد اعطت المحاكاة العددية بواسطة طريقة XEFGM نتائج دقيقة عن طريق عدد أقل من العقد (DOFs) بالمقارنة مع FEM التقليدية تحت حمل مزدوج وغير متناسب. وقد تم مقارنة النتائج مع مصادر ذات علاقة . تم استخدام برنامج الماتلاب في استخراج نتائج هذا البحث .

NOMENCLATURE :-

Symbol	Description	Unit
b	Vector of External Body Forces in x, y, and z Directions	---
B	Matrix of Derivatives of Shape Function	---
B_i^a	Matrix of Derivatives of Enrichment (Heaviside) Derivatives of Shape Functions	---
B_i^b	Matrix of Derivatives of Enrichment (Crack Tip) Derivatives of Shape Functions	---
B_i^u	Strain -Displacement Matrix (Derivatives of Shape Functions)	---
B_i^r	Strain -Displacement Matrix (Derivatives of Shape Functions)	---
c	Damping Coefficient	N/m.s
c_{ijkl}	Constitutive Tensor; i , j , k, l=1,2,3	---
D	Matrix Of Material Constants	---
E	Young's Modulus	GPa
J	Path-Independent J Integral for the Actual field	N/m
k	Kolosov Constant	---
K	Stiffness Matrix	---
K_I	Mode I Stress Intensity Factor	$MPa\sqrt{m}$
K_{II}	Mode II Stress Intensity Factor	$MPa\sqrt{m}$
K_{ij}^{rs}	Stiffness Matrix Components	---
L	Matrix Differential(Differential Operator Matrix)	---
MI	Local Interaction Integral	N/m
s_{ijkl}	Compliance Tensor; i , j , k, l=1,2,3	---
$u = \{u_1, u_2\}$	Near Tip Displacement field	m
u_1, u_2	Displacement Field Near Crack Tip	m
u_x, u_y	x and y Displacement Components	m
W^{ext}	Virtual Work of External Loading	J
W^{int}	Internal Virtual Work	J
Γ_t	Traction Boundary Condition	---
Γ_u	Displacement Boundary Condition	---
δ_{ij}	Kronecker Delta; i , j =1,2	---
ε	Strain Displacement	---
ε_{ij}	Strain Components	---
σ_{ij}	Stress Components	N/m ²
δ	Variation of Function	---
σ	Stress Tensor	---
ρ	Mass Density	kg/m^3
$\phi(x)$	Level Set Function	---

INTRODUCTION :-

Today, functionally graded materials (FGMs) are significant in many branches of engineering applications including aerospace, automobile, medical equipments, turbine industries, etc.

A formulated concept of functionally graded materials (FGMs) was proposed in 1984 by material scientists in Sendai, Japan, as a mean of preparing thermal barrier materials, and followed by a coordinated research in that country since 1986. FGMs are gradually replacing layered composites in the different applications from high-tech industries to rather ordinary devices Shiota and Miyamoto [1996].

Several studies have been performed on fracture analysis of functionally graded materials. Most of studies on these types of materials have been conducted by using the numerical methods rather than the theoretical methods due to inability to analytically investigate such complicated problems. In calculation of the stress intensity factors in isotropic FGMs, the order of singularity of the stress field in the vicinity of the crack tip was assumed the same as isotropic homogenous materials Delale and Erdogan [1983]. Dolbow and Gosz [2003] presented an approach that was applicable to the analysis of FGMs in which the form of the asymptotic near-tip fields matched those of a homogeneous material. In the derivation, an interaction energy contour integral was expressed in the domain form and evaluated as a post processing step in XFEM. Rao and Rahman [2003] used the meshless EFGM method for calculating the fracture parameters of isotropic FGM by developing two interaction integrals in terms of homogenous and non-homogenous auxiliary fields. In addition, Kim and Paulino [2003] developed an accurate scheme for evaluating mixed-mode SIFs by means of the interaction integral (M-integral) within FEM considering arbitrarily oriented straight and curved cracks in two-dimensional (2D) orthotropic FGMs. The interaction integral proved to be an accurate and robust scheme in the numerical problems where various types of material gradation, such as exponential, radial, and hyperbolic-tangent, might exist. They observed that the material orthotropy, material gradation and the direction of material gradation could have a significant influence on SIFs. Also, Kim and Paulino [2005] provided a critical assessment and comparison of three different formulations: non-equilibrium, incompatibility, and constant-constitutive-tensor formulations for calculation of stress intensity factor in FGMs by the interaction integral approach. Dai et al [2004] used a meshfree model for the static and dynamic analyses of FGM plates based on the radial point interpolation method (PIM). In this method, the mid-plane of FGM plate was represented by a set of distributed nodes while the material properties across the thickness were computed analytically to take into account their continuous variations from one surface to another Dai et al [2004].

Khazal et al [2016] used an extended element free galerkin method for liner elastic fracture analysis of functionally graded materials (FGMs). In addition, Gao et al [2008] presented 2D crack analysis in non-homogeneous isotropic and linear elastic FGMs by a boundary-domain integral formulation. Asadpoure et al [2006] presented modeling crack in orthotropic media using coupled finite element and partition of unity methods.

Motamedi and Mohammadi [2010] studied the dynamic behavior of fixed and moving cracks in orthotropic media using the extended finite element method. Also, delamination analysis of composites by new orthotropic bimaterial extended finite element method was performed by Ashari and Mohammadi [2013]. Similarly, Ghorashi et al [2012] presented a novel XIGA approach based on the combination of isogeometric analysis (IGA) and extended FEM for fracture analysis of structures. Bayesteh and Mohammadi [2013], clearly presented the efficiency of orthotropic XFEM in crack analysis of isotropic and anisotropic functionally graded materials.

One of the most well-known meshfree methods is the Element Free Galerkin (EFG) method Belytschko et al [1994], which uses the Moving Least Squares (MLS) approximation for generating the shape functions of required order of continuity. Being

free from the restrictions of mesh-based methods, such as FEM, EFG can be used more efficiency to solve complicated problems such as discontinuities, considerable meshing and re-meshing practices in structural optimization problems, or having multi domains of influence in multi physics problems. It is very difficult and sometimes impossible to completely overcome those mesh-related difficulties by a mesh-based method Chen et al [2006]. In this study, the development of extended EFGM for fracture analysis of cracked isotropic and orthotropic functionally graded materials (FGMs) is presented. The sub-triangular technique near the crack tip, modified support domain in the location of the crack tip, effective nodal distribution for the local crack region and for the whole geometry, and interaction integral method (M-integral) with the incompatibility form to calculate SIFs are explained in detail.

CONSTITUTIVE EQUATIONS :-

The Hooke's law for 2D elastic solids has the following form:

$$\boldsymbol{\sigma} = \mathbf{D}\boldsymbol{\varepsilon} \tag{1}$$

where \mathbf{D} is the matrix of material constants.

For isotropic non-homogenous materials (FGMs), \mathbf{D} can be defined as,

$$\mathbf{D} = \frac{E(x)}{1-\nu^2} \begin{bmatrix} 1 & \nu(x) & 0 \\ \nu & 1 & 0 \\ 0 & 0 & (1-\nu(x))/2 \end{bmatrix} \text{ (Plane stress)} \tag{2}$$

and

$$\mathbf{D} = \frac{E(x)(1-\nu(x))}{(1+\nu(x))(1-2\nu(x))} \begin{bmatrix} 1 & \frac{\nu(x)}{1-\nu(x)} & 0 \\ \frac{\nu(x)}{1-\nu(x)} & 1 & 0 \\ 0 & 0 & \frac{1-2\nu(x)}{2(1-\nu(x))} \end{bmatrix} \text{ (Plane strain)} \tag{3}$$

$E(x)$ and $\nu(x)$ in equations (2-3) can be viewed as smoothly varying ‘‘effective’’ material properties of FGMs. This change in the material properties cannot be easily implemented in analysis of anisotropic materials by many existing numerical methods.

For isotropic materials in the plane stress state, equation (1) can be converted to:

$$\boldsymbol{\varepsilon} = \mathbf{C}\boldsymbol{\sigma} = \begin{bmatrix} c_{11} & c_{12} & c_{16} \\ c_{12} & c_{22} & c_{26} \\ c_{16} & c_{26} & c_{66} \end{bmatrix} \begin{Bmatrix} \sigma_{xx} \\ \sigma_{yy} \\ \sigma_{xy} \end{Bmatrix} \tag{4}$$

where \mathbf{C} is the compliance matrix. \mathbf{C} for orthotropic plane stress problems can be written as:

$$\mathbf{C} = \begin{bmatrix} \frac{1}{E_1} & -\frac{\nu_{12}}{E_1} & 0 \\ -\frac{\nu_{12}}{E_1} & \frac{1}{E_2} & 0 \\ 0 & 0 & \frac{1}{G_{12}} \end{bmatrix} \tag{5}$$

CRACK TIP ASYMPTOTIC SOLUTION :-

Figure (1) defines a 2D orthotropic cracked body subjected to typical forces with relevant boundary condition, and definitions of global, local, and polar coordinates. The characteristic equation, obtained from the equilibrium and compatibility, be written as Asadpoure, Mohammadi [2007] and Lekhnitskii [1963]

$$c_{11}s^4 - 2c_{16}s^3 + (2c_{12} + c_{66})s^2 - 2c_{26}s + c_{22} = 0 \tag{6}$$

where c_{ij} are the components of the compliance matrix C .

The two dimensional displacement and stress fields in the vicinity of the crack tip are defined in terms of the roots $s_k = s_{kx} + is_{ky}; k = 1,2$ Sih et al [1965]:

- Mode I

$$u_1^I = K_I \sqrt{\frac{2r}{\pi}} \operatorname{Re} \left[\frac{1}{s_1 - s_2} (s_1 p_2 \sqrt{\cos\theta + s_2 \sin\theta} - s_2 p_1 \sqrt{\cos\theta + s_1 \sin\theta}) \right] \tag{7}$$

$$u_2^I = K_I \sqrt{\frac{2r}{\pi}} \operatorname{Re} \left[\frac{1}{s_1 - s_2} (s_1 q_2 \sqrt{\cos\theta + s_2 \sin\theta} - s_2 q_1 \sqrt{\cos\theta + s_1 \sin\theta}) \right] \tag{8}$$

$$\sigma_{xx}^I = \frac{K_I}{\sqrt{2\pi r}} \operatorname{Re} \left[\frac{s_1 s_2}{s_1 - s_2} \left(\frac{s_2}{\sqrt{\cos\theta + s_2 \sin\theta}} - \frac{s_1}{\sqrt{\cos\theta + s_1 \sin\theta}} \right) \right] \tag{9}$$

$$\sigma_{yy}^I = \frac{K_I}{\sqrt{2\pi r}} \operatorname{Re} \left[\frac{1}{s_1 - s_2} \left(\frac{s_1}{\sqrt{\cos\theta + s_2 \sin\theta}} - \frac{s_2}{\sqrt{\cos\theta + s_1 \sin\theta}} \right) \right] \tag{10}$$

$$\sigma_{xy}^I = \frac{K_I}{\sqrt{2\pi r}} \operatorname{Re} \left[\frac{s_1 s_2}{s_1 - s_2} \left(\frac{1}{\sqrt{\cos\theta + s_1 \sin\theta}} - \frac{1}{\sqrt{\cos\theta + s_2 \sin\theta}} \right) \right] \tag{11}$$

- Mode II

$$u_1^{II} = K_{II} \sqrt{\frac{2r}{\pi}} \operatorname{Re} \left[\frac{1}{s_1 - s_2} (p_2 \sqrt{\cos\theta + s_2 \sin\theta} - p_1 \sqrt{\cos\theta + s_1 \sin\theta}) \right] \tag{12}$$

$$u_2^{II} = K_{II} \sqrt{\frac{2r}{\pi}} \operatorname{Re} \left[\frac{1}{s_1 - s_2} (q_2 \sqrt{\cos\theta + s_2 \sin\theta} - q_1 \sqrt{\cos\theta + s_1 \sin\theta}) \right] \tag{13}$$

$$\sigma_{xx}^{II} = \frac{K_{II}}{\sqrt{2\pi r}} \operatorname{Re} \left[\frac{1}{s_1 - s_2} \left(\frac{s_2^2}{\sqrt{\cos\theta + s_2 \sin\theta}} - \frac{s_1^2}{\sqrt{\cos\theta + s_1 \sin\theta}} \right) \right] \tag{14}$$

$$\sigma_{yy}^{II} = \frac{K_{II}}{\sqrt{2\pi r}} \operatorname{Re} \left[\frac{1}{s_1 - s_2} \left(\frac{1}{\sqrt{\cos\theta + s_2 \sin\theta}} - \frac{1}{\sqrt{\cos\theta + s_1 \sin\theta}} \right) \right] \tag{15}$$

$$\sigma_{xy}^{II} = \frac{K_{II}}{\sqrt{2\pi r}} \operatorname{Re} \left[\frac{1}{s_1 - s_2} \left(\frac{s_1}{\sqrt{\cos\theta + s_1 \sin\theta}} - \frac{s_2}{\sqrt{\cos\theta + s_2 \sin\theta}} \right) \right] \tag{16}$$

where Re represents the real part of the statement, K_I and K_{II} are the stress intensity factors for mode I and mode II, respectively, and p_i, q_i are defined as:

$$p_i = c_{11} s_i^2 + c_{12} - c_{16} s_i \quad i = 1,2 \tag{17}$$

$$q_i = c_{12} s_i^2 + \frac{c_{22}}{s_i} - c_{26} \quad i = 1,2 \quad (18)$$

In FGMs (Figure (1)), the material properties, such as the modulus of elasticity E and the Poisson's ratio ν , vary in different points of the domain. Nevertheless, due to the fact that the linear-elastic singular stress field near the crack tip cannot be analytically obtained for general FGM problems, it is common to assume the field functions similar to homogenous media based on the crack tip material properties Rao and Rahman [2003]. Similarly, the displacements and stresses of a cracked orthotropic FGM are obtained from equations (17-18) by calculating the roots of the characteristic equation (6) at the crack tip.

COMPUTATION OF STRESS INTENSITY FACTORS BY THE INTERACTION INTEGRAL :-

Various forms of the interaction integral have been used to obtain the stress intensity factors (SIFs), including the non-equilibrium, the incompatibility, and the constant-constitutive-tensor formulations, as proposed by Kim and Paulino[6]. In the present work, the incompatibility formulation is employed to approximate the J-integral because it requires less complicated derivatives with more or less the same level of accuracy as the non-equilibrium formulation Kim, Paulino [2005] and Hosseini et al [2013] . The incompatibility formulation is based on the following relations for the auxiliary fields

$$\sigma_{ij} = d_{ijkl}(x)\varepsilon_{kl} , \quad \varepsilon_{ij} \neq \frac{1}{2}(u_{i,j} + u_{j,i}) , \quad \sigma_{ij,j} = 0 \quad (19)$$

where d_{ijkl} is the material modulus. The material compliance tensor c_{ijkl} can be obtained from the first relation of Eq. (19)

$$\varepsilon_{ij} = c_{ijkl}(x)\sigma_{kl} \quad (i,j,k,l=1,2,3) \quad (20)$$

Coefficients c_{ijkl} are related to components of the material compliance tensor c_{ij} .

$$\begin{bmatrix} c_{11} & c_{12} & c_{16} \\ c_{12} & c_{22} & c_{26} \\ c_{16} & c_{26} & c_{66} \end{bmatrix} = \begin{bmatrix} c_{1111} & c_{1122} & 2c_{1112} \\ c_{2211} & c_{2222} & 2c_{2212} \\ 2c_{1211} & 2c_{26} & 4c_{1212} \end{bmatrix} \quad (21)$$

The equivalent domain formulation of the J-integral for an arbitrary contour Γ surrounding the crack tip can be expressed as (Figure (2))

$$J = \int_A (\sigma_{ij}u_{i,1} - w\delta_{1j})q_{,j}dA + \int_A (\sigma_{ij}u_{1,i} - w\delta_{1j})_{,j}qdA \quad (22)$$

where q is a smooth function varying from q=1 on the interior boundary of surface A to q=0 on the outer one. n_j is the j th component of the outward unit normal to Γ , δ_{ij} is the Kronecker delta and the local Cartesian coordinate system x_1 is set parallel to the crack surface. w is the strain energy density,

$$w = \frac{1}{2} \sigma_{ij} \varepsilon_{ij} \quad (23)$$

The interaction integral method is applied to calculate the mode I and II stress intensity factors. The interaction integral can be defined as Guo et al [2012]:

$$M = \int_A \left\{ \sigma_{ij} u_{i,1}^{aux} + \sigma_{ij}^{aux} u_{i,1} - \frac{1}{2} (\sigma_{ik} \varepsilon_{ik}^{aux} + \sigma_{ik}^{aux} \varepsilon_{ik}) \delta_{1j} \right\} q_j dA + \int_A \left\{ \sigma_{ij} (c_{ijkl}^{tip} - c_{ijkl}(x)) \sigma_{kl,1}^{aux} \right\} q dA \quad (24)$$

The effect of two superimposed fields can be written as Kim and Paulino [2002]

$$M = 2t_{11} K_I^{aux} K_I + t_{12} (K_I^{aux} K_{II} + K_{II}^{aux} K_I) + 2t_{22} K_{II}^{aux} K_{II} \quad (25)$$

with

$$t_{11} = -\frac{c_{22}}{2} Im \left(\frac{s_1 + s_2}{s_1 s_2} \right) \quad (26)$$

$$t_{12} = -\frac{c_{22}}{2} Im \left(\frac{1}{s_1 s_2} \right) + \frac{c_{11}}{2} Im(s_1 s_2) \quad (27)$$

$$t_{22} = -\frac{c_{11}}{2} Im(s_1 + s_2) \quad (28)$$

Substituting $K_I^{aux} = 1, K_{II}^{aux} = 0$ and $K_I^{aux} = 0, K_{II}^{aux} = 1$ into equation (25), results in the following simplified simultaneous equations

$$M_1 = 2t_{11} K_I + t_{12} K_{II} \quad (K_I^{aux} = 1, K_{II}^{aux} = 0) \quad (29)$$

$$M_2 = t_{12} K_I + 2t_{22} K_{II} \quad (K_I^{aux} = 0, K_{II}^{aux} = 1)$$

which should be solved for calculation of the actual modes I and II stress intensity factors. In this work, maximum energy release rate criteria are implemented for crack propagation. SIF values in terms of crack propagation angle is represented by Hosseini et al [2013].

EFG FORMULATION :-

Figure (3) shows a two-dimensional problem of linear elasticity which includes a crack Γ_c . The partial differential equation of this problem can be written in the form of, Equilibrium equation : $L^T \sigma + b = 0$ in Ω (30)

with the following boundary conditions:

$$\text{Natural boundary condition : } \sigma n = \bar{t} \text{ on } \Gamma_t \quad (31)$$

$$\text{Essential boundary conditionaluminium : } u = \bar{u} \text{ on } \Gamma_u \quad (32)$$

$$\text{Tracttion free crack : } \sigma n = 0 \text{ on } \Gamma_c \quad (33)$$

where L is the differential operator defined as

$$L = \begin{bmatrix} \frac{\partial}{\partial x} & 0 \\ 0 & \frac{\partial}{\partial y} \\ \frac{\partial}{\partial y} & \frac{\partial}{\partial x} \end{bmatrix} \quad (34)$$

and σ, u and b are the stress, displacement and body force vectors, respectively. \bar{t} is the prescribed traction on the traction (natural) boundary; \bar{u} is the prescribed displacement on

the displacement (essential) boundary and \mathbf{n} is the unit outward normal vector at a point on the natural boundary. Since the MLS shape functions lack the Kronecker delta function property, the Lagrange multiplier technique is adopted to enforce the essential (displacement) boundary conditions. The constrained weak form of the governing equation can be written as:

$$\int_{\Omega} (\mathbf{L}\delta\mathbf{u})^T (\mathbf{D}\mathbf{L}\mathbf{u})d\Omega - \int_{\Omega} \delta\mathbf{u}^T \mathbf{b}d\Omega - \int_{\Gamma_t} \delta\mathbf{u}^T \bar{\mathbf{t}}d\Gamma - \int_{\Gamma_u} \delta\boldsymbol{\lambda}^T (\mathbf{u} - \bar{\mathbf{u}})d\Gamma - \int_{\Gamma_u} \delta\mathbf{u}^T \boldsymbol{\lambda}d\Gamma = 0 \quad (35)$$

where \mathbf{D} is the matrix of elastic constants (inverse of compliance matrix \mathbf{c}), and $\boldsymbol{\lambda}$ is the Lagrange multiplier variable. The problem domain is now represented by a set of n field nodes in order to approximate the displacement variable. EFG uses the moving least squares (MLS) shape functions Lancaster and Salkauskas [1981] to approximate the displacement at any point of interest using a set of nodes in the local support domain of that point. The MLS shape function associated with the node i a point \mathbf{x} can be written as Liu [2010],

$$\phi_i(\mathbf{x}) = \mathbf{p}^T(\mathbf{x})[\mathbf{A}(\mathbf{x})]^{-1}w(\mathbf{x} - \mathbf{x}_i)\mathbf{p}(\mathbf{x}_i) \quad (36)$$

where $\mathbf{p}(\mathbf{x})$ is the basis function. A linear basis function is adopted in this study,

$$\mathbf{p}^T(\mathbf{x}) = [1 \ x \ y] \quad (37)$$

and \mathbf{A} is defined as,

$$\mathbf{A}(\mathbf{x}) = \sum_{i=1}^n w(\mathbf{x} - \mathbf{x}_i) \mathbf{p}(\mathbf{x}_i)\mathbf{p}^T(\mathbf{x}_i) \quad (38)$$

where n is the number of nodes in the neighborhood of point \mathbf{x} where the weight function $w(\mathbf{x} - \mathbf{x}_i) \neq 0$. The commonly used cubic spline weight function is used here

$$w(r) = \begin{cases} \frac{2}{3}-4r^2+4r^3 & r \leq \frac{1}{2} \\ \frac{4}{3}-4r+4r^2-\frac{4}{3}r^3 & \frac{1}{2} < r \leq 1 \\ 0 & r > 1 \end{cases} \quad (39)$$

where r_s is the radius of the support domain for node i .

An efficient extrinsic enrichment, similar to XFEM, is adopted to account for discontinuities or singularities within the support domain. The extrinsically enriched displacement approximation for a typical point \mathbf{x} can be written as Mohammadi [2007]:

$$\mathbf{u}^h(\mathbf{x}) = \sum_{i=1}^n \phi_i(\mathbf{x})\mathbf{u}_i + \sum_{k=1}^{m_t} \phi_k \sum_{\alpha=1}^4 Q_{\alpha}(\mathbf{x})\mathbf{b}_k \quad (40)$$

where \mathbf{b}_k is the vector of additional degrees of freedom for modeling crack tips m_t , is the set of nodes that the discontinuity is in its influence (support) domain and $Q_{\alpha}(\mathbf{x})$ are the enrichment functions. The first term in the right-hand side of Eq. (40) is the classical EFG approximation to determine the displacement field, while the second term is the enrichment approximation in order to accurately represent the analytical solution near the crack tip. The orthotropic enrichment functions (that will be used in Eq. (40)) are used extrinsically for anisotropic materials to enrich the MLS formulation Mohammadi [2012]:

$$Q(r, \theta) = \left(\sqrt{r} \cos\left(\frac{\theta_1}{2}\right) \sqrt{g_1(\theta)}, \sqrt{r} \cos\left(\frac{\theta_2}{2}\right) \sqrt{g_2(\theta)}, \sqrt{r} \sin\left(\frac{\theta_1}{2}\right) \sqrt{g_1(\theta)}, \sqrt{r} \sin\left(\frac{\theta_2}{2}\right) \sqrt{g_2(\theta)} \right) \quad (41)$$

where

$$\theta_j = \arctan\left(\frac{s_{jy} \sin(\theta)}{\cos(\theta) + s_{jx} \sin(\theta)}\right) \quad (j=1,2) \quad (42)$$

$$g_j(\theta) = \sqrt{(\cos(\theta) + s_{jx} \sin(\theta))^2 + (s_{jy} \sin(\theta))^2} \quad (43)$$

where $s_j = s_{jx} + i s_{jy}$ are the roots of the characteristic equation (6).

Discretization of Eq. (35) results in

$$\begin{bmatrix} \mathbf{K} & \mathbf{Q} \\ \mathbf{Q}^T & \mathbf{0} \end{bmatrix} \begin{bmatrix} \mathbf{U} \\ \boldsymbol{\lambda} \end{bmatrix} = \begin{bmatrix} \mathbf{F} \\ \mathbf{q} \end{bmatrix} \quad (44)$$

where \mathbf{K} is the global stiffness matrix, \mathbf{F} is the global force vector, \mathbf{Q} and \mathbf{q} are the Lagrange related terms for enforcement of the boundary conditions by the Lagrange multipliers $\boldsymbol{\lambda}$,

$$\mathbf{Q} = - \int_{\Gamma_u} \mathbf{N}^T \boldsymbol{\phi} d\Gamma \quad (45)$$

$$\mathbf{q} = - \int_{\Gamma_u} \mathbf{N}^T \bar{\mathbf{u}} d\Gamma \quad (46)$$

$$\boldsymbol{\lambda}(\mathbf{x}) = \sum_{i=1}^{n_\lambda} N_i(\mathbf{x}) \lambda_i \quad (47)$$

where \mathbf{N} is the Lagrange interpolation shape functions over the boundary Γ_u with n_λ nodes. \mathbf{U} is the global displacement vector that collects the displacements of all nodes in the entire problem domain and additional enrichment degrees of freedom:

$$\mathbf{U} = \{\mathbf{u} \quad \mathbf{b}_1 \quad \mathbf{b}_2 \quad \mathbf{b}_3 \quad \mathbf{b}_4\}^T \quad (48)$$

\mathbf{K} and \mathbf{F} are assembled from the nodal stiffness matrix and nodal force vector, respectively:

$$\mathbf{K}_{ij}^n = \begin{bmatrix} K_{ij}^{uu} & K_{ij}^{ub} \\ K_{ij}^{bu} & K_{ij}^{bb} \end{bmatrix} \quad (49)$$

$$\mathbf{F}_i^n = \{\mathbf{F}_i^u \quad \mathbf{F}_i^{b1} \quad \mathbf{F}_i^{b2} \quad \mathbf{F}_i^{b3} \quad \mathbf{F}_i^{b4}\}^T \quad (50)$$

where

$$\mathbf{K}_{ij}^{rs} = \int_{\Omega} (\mathbf{B}_i^r)^T \mathbf{D} \mathbf{B}_j^s d\Omega \quad (r, s = u, b) \quad (51)$$

$$\mathbf{F}_i^u = \int_{\Omega} \phi_i^t \mathbf{b} d\Omega + \int_{\Gamma_t} \phi_i^T \bar{\mathbf{t}} d\Gamma \quad (52)$$

$$\mathbf{F}_i^{ba} = \int_{\Omega} \phi_i^T Q_a \mathbf{b} d\Omega + \int_{\Gamma_t} \phi_i^T Q_a \bar{\mathbf{t}} d\Gamma \quad (a = 1,2,3,4) \quad (53)$$

B_i^u and B_i^b are matrices of shape function derivatives,

$$B_i^u = \begin{bmatrix} \phi_{i,x} & 0 \\ 0 & \phi_{i,y} \\ \phi_{i,y} & \phi_{i,x} \end{bmatrix} \quad (54)$$

$$B_i^b = [B_i^{b1} \quad B_i^{b2} \quad B_i^{b3} \quad B_i^{b4}] \quad (55)$$

$$B_i^u = \begin{bmatrix} (\phi_i Q_\alpha)_x & 0 \\ 0 & (\phi_i Q_\alpha)_y \\ (\phi_i Q_\alpha)_y & (\phi_i Q_\alpha)_x \end{bmatrix} \quad (\alpha = 1,2,3,4) \quad (56)$$

Strain and stress components can then be retrieved from nodal displacements u^h using Eqs. (57) and (58), respectively,

$$\varepsilon = Lu^h \quad (57)$$

$$\sigma = D\varepsilon \quad (58)$$

Appropriate Domain of Influence

Among many available techniques to account for discontinuous fields across the crack Ghorashi et al [2011], selection of the suitable support domain near a crack face is performed as illustrated in Figure (4-a). For each point x_1 , the nodes on the opposite side of the crack face are not considered. In order to take into account the effect of discontinuity near a crack tip x_c , indirect distance of $s_1 + s_2(\mathbf{x})$ is considered instead of the direct distance of $s_0(\mathbf{x})$, as shown in Figure (4-b).

$$\begin{cases} s_0(\mathbf{x}) = \|\mathbf{x} - \mathbf{x}_1\| \\ s_1(\mathbf{x}) = \|\mathbf{x}_1 - \mathbf{x}_c\| \\ s_2(\mathbf{x}) = \|\mathbf{x} - \mathbf{x}_c\| \end{cases} \quad (59)$$

Numerical Integration by the Sub-Triangle Technique

Usually the Gauss quadrature rule is employed for numerical integration inside the background cell of the EFG mesh free method. Existence of a discontinuity within a background cell may result in substantial accuracy reduction. Many researchers demonstrated that a regular increase in the order of Gauss integration does not necessarily improve the accuracy of integration over a discontinuous element/cell, whereas independent integration of each side of the discontinuity with even low order rules does guarantee an accurate integration Ghorashi et al [2011]. So, an efficient technique is required to define the necessary points needed for the integration within these background cells, while remains consistent with the crack geometry. An approach similar to the one proposed by Dolbow [1999] and originally utilized by Ghorashi et al [2011] is adopted. Any background cell which intersects with a crack is subdivided at both sides into sub-triangles whose edges are adapted to the crack faces, as illustrated in Figure (5). It is important to note that, while triangulation of the crack tip element substantially improves the accuracy of integration by increasing the order of Gauss quadrature, it also avoids numerical complications of singular fields at the crack tip because none of the Gauss points are placed on the position of the crack tip.

NUMERICAL CASE STUDY :-

Fracture analysis in a graded glass/epoxy beam subjected to three point bending is presented in this section to illustrate the application of EFG mesh free method for crack analysis of functionally graded materials (FGMs). In addition, the sub-triangular technique near the crack tip, appropriate support domain in the location of the crack and crack tip, the proper nodal distribution for local crack region and for the whole geometry, and the interaction integral method with the incompatibility formulation are adopted to calculate SIFs for cracked FGMs. Figure (10) shows geometry and boundary conditions of the simply supported FGM beam. **Rousseau and Tippur [2000]** have used dimensionless parameter ξ which is zero at the left edge of graded portion and one at the right one. Modulus of elasticity, Poisson's ratio and critical SIFs in the graded domain are presented in Table 1. The two edge cracks are emanated from the lower edge at $\xi = 0.17$ and $\xi = 0.58$. The distribution of 2070 non-uniform nodes, and a 64×28 background mesh are used for simulation of the problem that can be shown in Figure (6) at $\xi = 0.17$. The integration of each sub-triangle cell is performed by 13 Gauss points nearby the crack and for other cells; a 2×2 Gauss quadrature rule is used. Enrichment and split nodes around the crack and crack tip can depict in Figure (7). **Rousseau and Tippur [2000]** also modeled their specimen by ANSYS using 10,000 eight-noded elements and 30,000 nodes. Also, Bayesteh and Mohammadi [17] solved this problem by using the extended finite element method on a mesh of 4848 three-node elements and 2547 nodes to extract the final results. In addition, Kim and Paulino [2004] used typical mesh discretization that consists of 1067 Q8, 155 T6, and 12 T6qp elements, with a total of 1234 elements and 3725 nodes. The results of present work have good agreement with relevant references as depict in Table 2 and Table 3. The verification of the work can be illustrated in Table 4 and Figures (8-9). Finally, Figure (10) shows the comparison of the effect of crack increment length on crack trajectory for present work with experimental work Rousseau and Tippur [2000] at $\xi = 0.17$, 0.58 , and $\xi = 1.00$.

CONCLUSIONS :-

Development of the XEFGM method for simulation of crack propagation of glass-filled epoxy beams and graded (along the X1 direction) beams with the use of the sub-triangle technique for numerical integration, appropriate support domain and the enrichment functions in the crack location for give significantly increasing in the accuracy of the solution. **The** triangulation technique substantially improves the accuracy of integration by increasing the order of Gauss quadrature, and avoids numerical complications of singular fields at the crack tip because none of the Gauss points are placed on the position of the crack tip. **The** use of the incompatible interaction integral method provides very accurate results for the values of SIFs in mixed mode fracture analysis of FGMs.

Table 1: Modulus of elasticity, Poisson’s ratio and critical SIF in graded domain of glass-filled epoxy.

ξ	E (MPa)	ν	K_{cr} (MPa \sqrt{m})
$0 \leq$	3000	0.35	1.2
0.17	3300	0.34	2.1
0.33	5300	0.33	2.7
0.58	7300	0.31	2.7
0.83	8300	0.3	2.6
$1 \geq$	8600	0.29	2.6

Table 2: $d_{max} = 2$ and $r_j = 1.2$.

ξ	K_I (MPa \sqrt{m})			K_{II} (MPa \sqrt{m})		
	Present work	[h]	[k]	Present work	[17]	[33]
0.17	2.087	2.087	2.088	-0.116	-0.117	-0.127
0.58	2.689	2.694	2.695	-0.087	-0.085	-0.094
1	2.588	-	2.598	-0.010	-	-0.013

Table 3: $d_{max} = 2$ and $r_j = 1.2$.

ξ	P_{cr} (N)			Crack initiation angle θ_0 (deg.)		
	Present work	[h]	[k]	Present work	[17]	[33]
0.17	255	250	249.3	6.901	7.009	7
0.58	298	300	298	4.020	3.998	4
1	295	-	289.9	0.601	-	0.5

Table 4: Average and maximum errors of SIFs (mode I) for different support domain size.

$\xi=0.17; r_j = 1.2$	d_{max}		
	1.7	2	2.3
K_I (MPa \sqrt{m})	2.081	2.087	2.091
K_{II} (MPa \sqrt{m})	-0.112	-0.116	-0.111

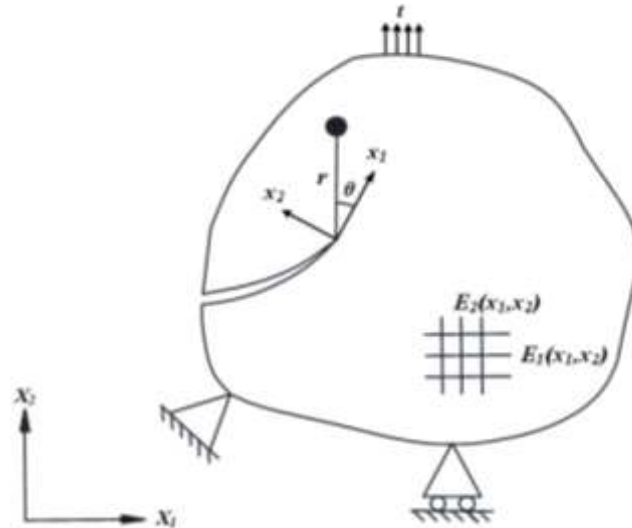


Figure (1) A cracked orthotropic FGM body.

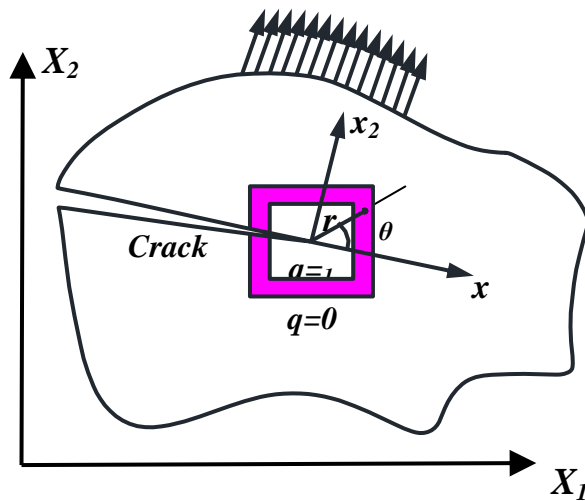


Figure (2) : The contour integral at the crack tip.

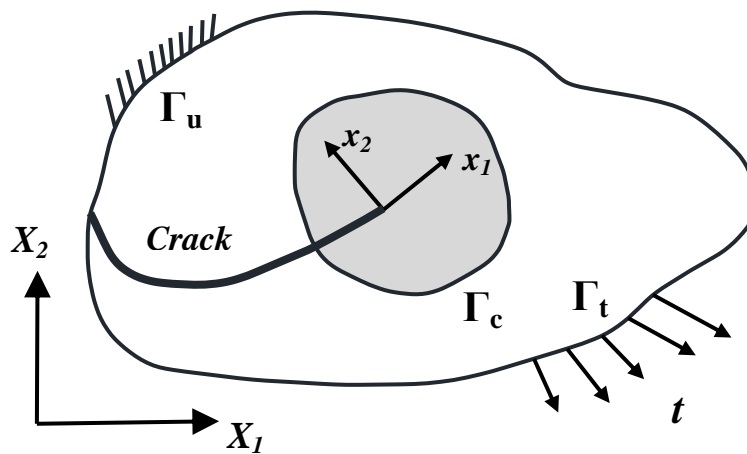


Figure (3) : A general two-dimensional cracked body.

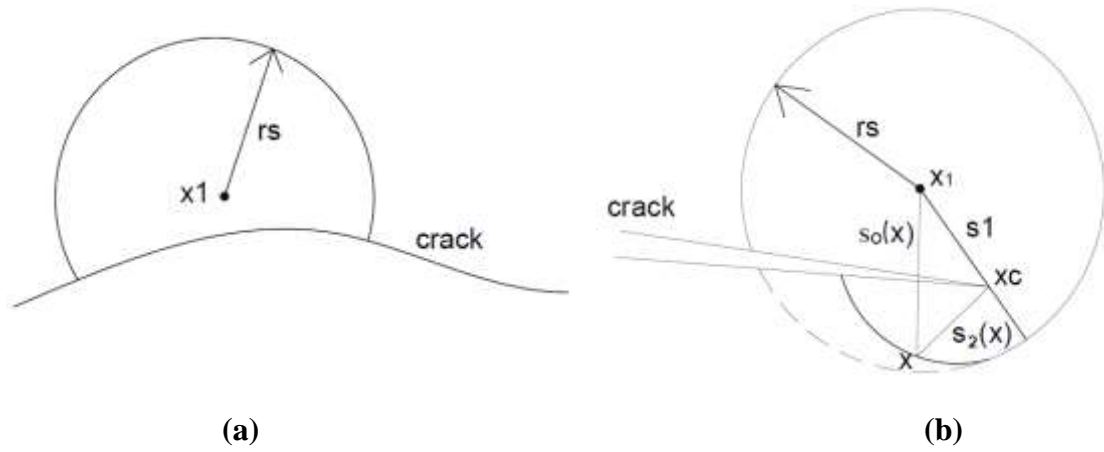


Figure (4) Selection of the support domain. (a) near a crack face, (b) near a crack tip. (r_s : radius of support domain)

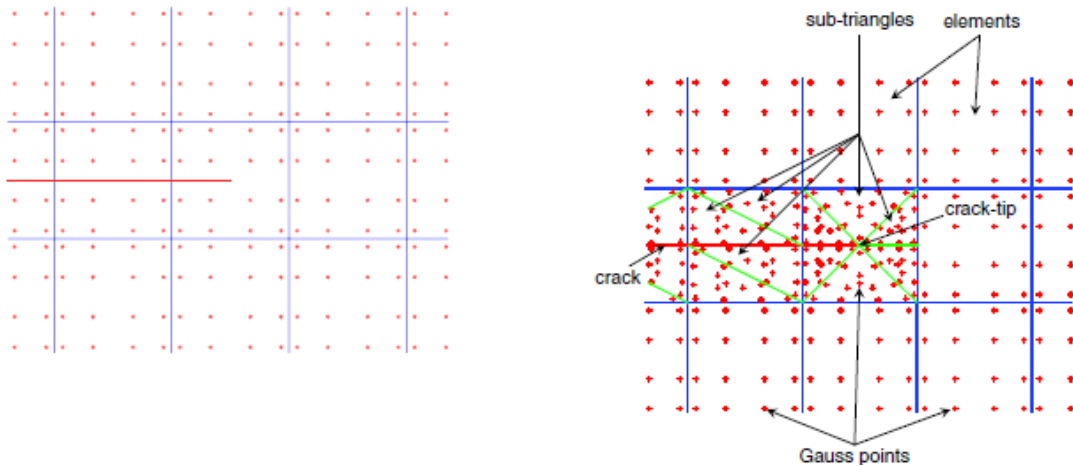


Figure (5): Distribution of Gauss points around the crack in the standard approach and the sub-triangles technique.

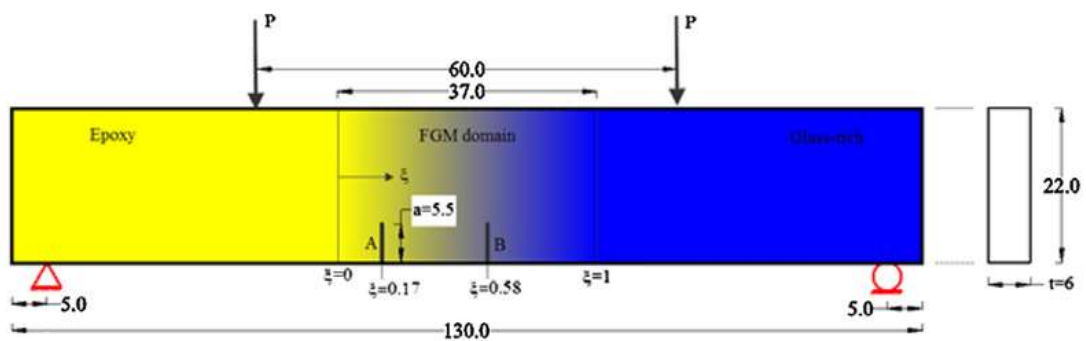
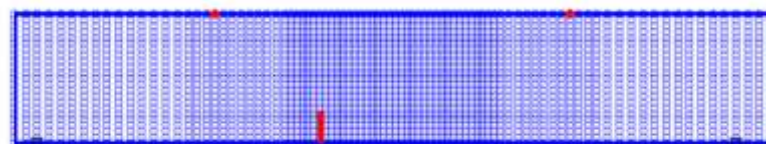
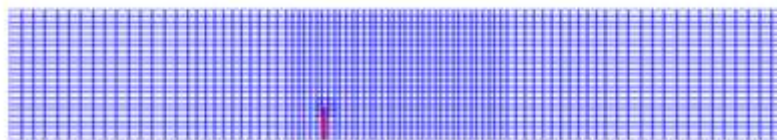


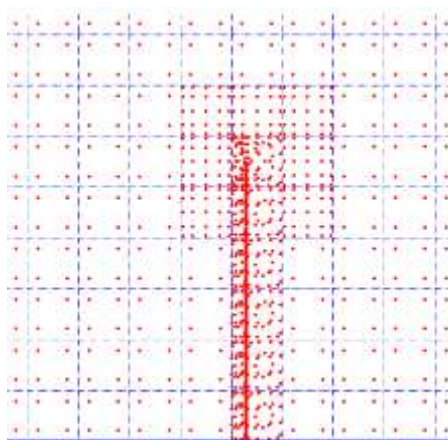
Figure (6): Crack in a graded glass/epoxy beam subjected to four point bending (the dimensions in mm)



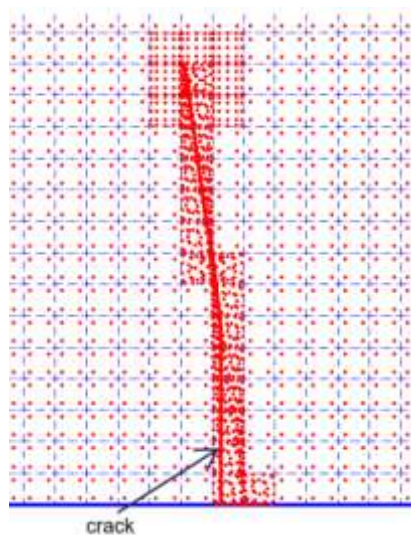
(a)



(c)



(b)



(c)

Figure (6): (a) Distribution of 2070 nonuniform nodes, (b) background cells, (c-d) Subtriangles technique at initial-propagation of crack.

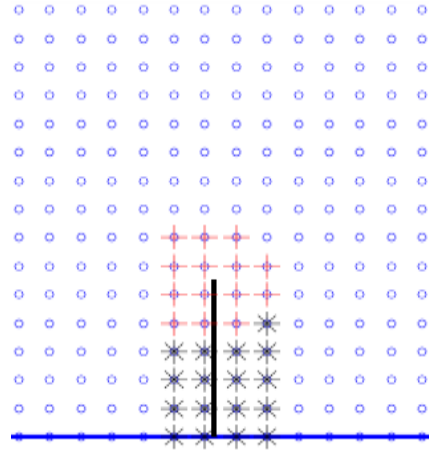


Figure (7) : Enrichment and split nodes around the crack and crack tip.

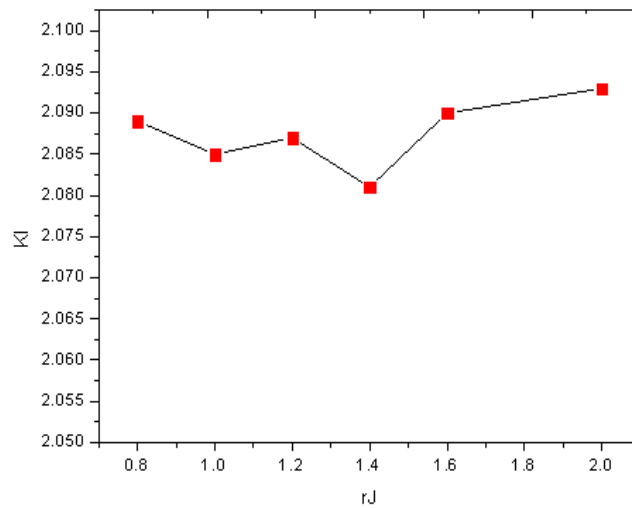


Figure (8) : Values of K_I (MPa \sqrt{m}) for various relative r_J .

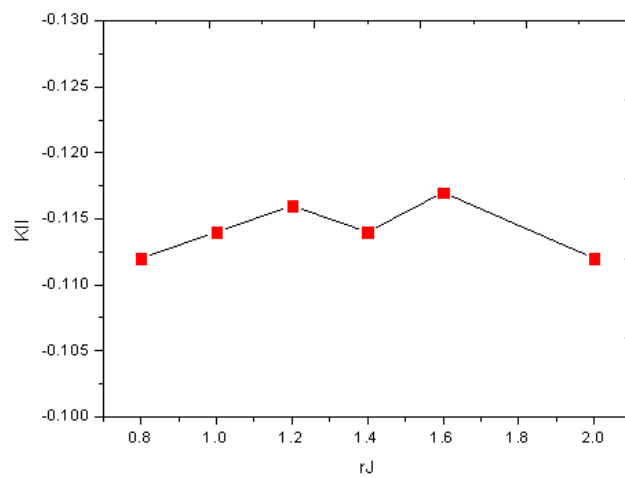


Figure (9) : Values of K_{II} (MPa \sqrt{m}) for various relative r_J .

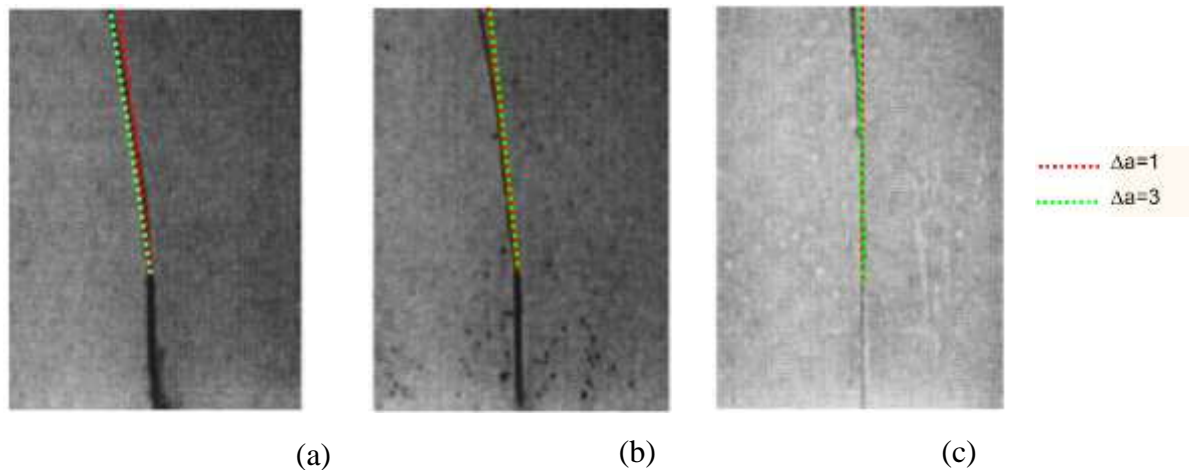


Figure (10): Comparison of the effect of crack increment length on crack trajectory for present work and experimental work [32]: (a) $\xi = 0.17$; (b) $\xi = 0.58$; (c) $\xi = 1.00$) of the crack in an FGM .

REFERENCES :-

- A. Asadpoure and S. Mohammadi, "Developing new enrichment functions for crack simulation in orthotropic media by the extended finite element method" *Int. J. Numer. Meth. Engng* 2007; 69:2150–2172
- A. Asadpoure, S. Mohammadi and A. Vafai, "Crack analysis in orthotropic media using the extended finite element method" *Thin-Walled Structures*, 44 (2006) 1031–1038.
- A. Asadpoure, S. Mohammadi and A. Vafai, "Modeling crack in orthotropic media using a coupled finite element and partition of unity methods" *Finite Elements in Analysis and Design* 42 (2006) 1165 – 1175.
- B.N. Rao and S. Rahman, "Mesh-free analysis of cracks in isotropic functionally graded materials" *Engineering Fracture Mechanics* 70 (2003) 1–27.
- D. Motamedi and S. Mohammadi, "Dynamic crack propagation analysis of orthotropic media by the extended finite element method" *International Journal of Fracture*, 161 (2010) 21-39.
- D. Motamedi and S. Mohammadi, "Fracture Analysis of Composites by Time Independent Moving-Crack Orthotropic XFEM" *International Journal of Mechanical Sciences*, 54 (2012) 20-37.
- D. Motamedi and S. Mohammadi, "Dynamic analysis of fixed cracks in composites by the extended finite element method" *Engineering Fracture Mechanics* 77 (2010) 3373–3393.
- F. Delale and F. Erdogan, "The crack problem for a non-homogeneous plate", *ASME Journal of Applied Mechanics*, 50(3), 609–614, 1983.

G.C. Sih, P.C. Paris and G.R. Irwin, "On cracks in rectilinearly anisotropic bodies" *International Journal of Fracture Mechanics* 1965; 1:189–203.

G.R. Liu, "Meshfree methods moving beyond the finite element method", second edition-2010 by Taylor and Francis Group, LLC.

H. Bayesteh and S. Mohammadi, "XFEM fracture analysis of orthotropic functionally graded materials" , *Journal of Composites, part B*, vol. 44, pp 8-25, 2013.

Haider Khazal, Hamid Bayesteh, Soheil Mohammadi, Sayyed Shahram Ghorashi, and Ameen Ahmed, "An extended element free Galerkin method for fracture analysis of functionally graded materials" *mechanics of advanced materials and structures* 23 (2016) 513-528.

I. Shiota and Y. Miyamoto, "Functionally graded materials 1996" Elsevier Science, Proceedings of the 4th international symposium on Functionally Graded Materials, AIST Tsukuba Research center, Tsukuba, Japan, October 21-24,1996.

J. Dolbow, "An extended finite element method with discontinuous enrichment for applied mechanics", Ph.D. thesis. Northwestern University, Evanston, IL, USA, 1999.

J.E. Dolbow and M. Gosz, "On the computation of mixed-mode stress intensity factors in functionally graded materials" *International Journal of Solids and Structures* 39 (2002) 2557–2574.

J.-H. Kim and G. H. Paulino, "An accurate scheme for mixed-mode fracture analysis of functionally graded materials using the interaction integral and micromechanics models" *International Journal For Numerical Methods In Engineering*, 2003; 58:1457–1497.

J.-H. Kim and G. H. Paulino, "Consistent Formulations of the Interaction Integral Method for Fracture of Functionally Graded Materials" *Journal of Applied Mechanics* ,ASME-May 2005, Vol. 72, pp 351-364

J.-H. Kim and G.H. Paulino, "Mixed-mode fracture of orthotropic functionally graded materials using finite elements and the modified crack closure method", *Engineering Fracture Mechanics*, 69 (14–16), 1557–1586, 2002.

J.-H. Kim and G.H. Paulino, "Simulation of crack propagation in functionally graded materials under mixed-mode and non-proportional loading" *International Journal of Mechanics and Materials in Design* 1: 63–94, 2004.

K. Y. Dai, G. R. Liu, K. M. Lim, X. Han and S. Y. Du, "A meshfree radial point interpolation method for analysis of functionally graded material (FGM) plates" *Computational Mechanics* 34 (2004) 213–223 ,Springer-Verlag 2004.

L. Guo, F. Guo, H. Yu and L. Zhang, "An interaction energy integral method for nonhomogeneous materials with interfaces under thermal loading" *International Journal of Solids and Structures* 49 (2012) 355–365.

P. Lancaster and K. Salkauskas "Surfaces Generated by Moving Least Squares Methods", Mathematics of Computation, Vol. 37, pp. 141-158, 1981

Rousseau, C.-E. and Tippur, H.V. "Compositionally graded materials with cracks normal to the elastic gradient". Acta Material 48(16), 4021–4033, (2000).

S. Esna Ashari and S. Mohammadi, "Delamination analysis of composites by new orthotropic biomaterial extended finite element method" International Journal For Numerical Methods In Engineering , 86(13) 1507 – 1543.

S. Mohammadi, "Extended finite element method For fracture analysis of structures" First Edition 2007-Blackwell Publishers, UK.

S. Mohammadi, "XFEM fracture analysis of composites", 2012, A John Wiley & Sons, Ltd. Publication.

S.G. Lekhnitskii, "Theory of an Anisotropic Elastic Body", Holden-Day: San Francisco, 1963.

S.S. Ghorashi, N. Valizadeh and S. Mohammadi, "Extended isogeometric analysis for simulation of stationary and propagating cracks" International Journal For Numerical Methods In Engineering (2011), 89, 9 (2012) 1069- 1101.

S.S. Ghorashi, S. Mohammadi and S.R.S. Yazdi , "Orthotropic enriched element free Galerkin method for fracture analysis of composites" Engineering Fracture Mechanics- Volume 78, Issue 9, June 2011, Pages 1906–1927.

S.S. Hosseini, H. Bayesteh and S. Mohammadi, "Thermo-mechanical XFEM crack propagation analysis of functionally graded materials" Materials Science and Engineering: A, Volume 561, 20 January 2013, Pages 285–302.

T. Belytschko, Y. Y. Lu and L. Gu , M. Fleming, and P. Krysl, "Element free Glarkin method" International journal for numerical method in engineering, vol.73, 229-256, 1994.

X.W. Gao, Ch. Zhang, J. Sladek and V. Sladek, "Fracture analysis of functionally graded materials by a BEM" Composites Science and Technology 68 (2008) 1209-1215.

Y. Chen, J. D. Lee and A. Eskandarian, "Meshless methods in solid mechanics", 2006 Springer Science and Business Media, Inc.